1983

The lateral response of an airship to turbulence

Layton, D.; Wrobleski, J. Jr

American Institute of Aeronautics and Astronautics (AIAA)

Layton, D., and J. Wrobleski Jr. "The lateral response of an airship to turbulence." 5th Lighter-Than Air Conference. 1983.
http://hdl.handle.net/10945/67012

83-1989

THE LATERAL RESPONSE OF AN AIRSHIP TO TURBULENCE

Donald M. Layton#
Naval Postgraduate School
Monterey, California

John J. Wrobleski, Jr.*
Lieutenant U. S. Navy
USS Dwight D. Eisenhower (CVN-69)

Abstract

A method is derived for finding the linear response and loading transfer functions for the lateral aerodynamic case of an airship flight through turbulence. The functions are in a form that can be applied to the various spectral analysis methods currently used by designers to predict survivability. The results show that the peak motion response and loading occur when the spectral component has a wavelength equal to the airship length, and that simple feedback of heading angle does not reduce this peak significantly.

Introduction

Turbulence is a prime cause for concern in the design and operation of Lighter-Than-Air (LTA) craft. The spectacular crashes of the airships Shenandoah and Macon are, perhaps, the most obvious reminders of the powerful effect that the wind can have on these somewhat fragile vehicles. It is imperative that proper consideration be given to the gust response of an airship, from both the viewpoints of dynamics and structures.

At the time of the early construction of the great rigids, designers had but a cursory knowledge of turbulence and how to deal with it. Burgess[1] devoted but one page to the subject, and that is chiefly a warning that gusts encountered in flight can place larger loads on an airship that any operational maneuver of which the vehicle is capable.

Gust predictions and representations have improved from the early statistical evaluations[2] of the simple ramp gust to spectral analysis of improved gust models, such as the (1 - cosine) gust. However, the improvement in gust modeling techniques has proceeded at a much more rapid pace than the application of these techniques to airship response. The work of Calligeros and McDavitt[3] in 1958 was the standard for airship response to turbulence until their technique was refined by DeLaurier and Hui[4], commencing in the late 1970's. The latter works, as well as most others dealing with this subject, concentrated mainly on the longitudinal aerodynamic case.

Professor and Acting Chairman, Dept. of Aeronautics, Associate Fellow AIAA
* Member AIAA

This paper applies the De Laurier model to the lateral case, thereby enabling the response to side-force to be calculated so that bending and shear in the horizontal plane can be taken into account.

Figure 1 shows the shape for a discrete (1 - cosine) gust, where W_m and d_m are the maximum gust velocity and distance along the flight path for this maximum.

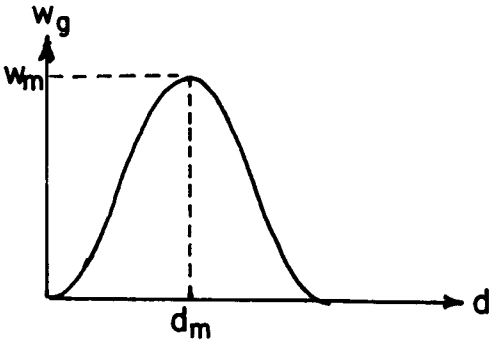

Fig. 1 The (1 - cosine) Gust Shape

The value for d_m, as prescribed by the Federal Aviation Administration (FAA), is $2d_m = 25\bar{c}$, where $\bar{c}$ is the characteristic longitudinal length of the vehicle. The $25\bar{c}$ wavelength was chosen because it historically couples with the short period pitch mode of a rigid aircraft to produce the largest load factors. Calligeros and McDavitt show that, for airships, the maximum loads occur when the wavelength is equal to the length of the airship.

The modeling of turbulence, because it is nonhomogeneous, non-stationary and anisotropic is quite complex, but simplifications can reduce the problems that this causes. It may be assumed that everywhere except in the planetary boundary layer (below 1,000 feet) the turbulence is homogeneous, i.e., the statistics of the field do not vary through space. In the boundary layer, while scale length and intensity are not homogenous in the vertical plane, they are essentially homogeneous in the horizontal plane. And, over the time intervals of interest to flight, it is not unreasonable to assume that the turbulence is statistically time constant, or 'stationary'.

One last simplification used to model atmospheric turbulence is Taylor's hypothesis of the 'frozen field'. The change in the velocity field perceived

by an aircraft as it passes with velocity U_o through the air is given as,

$$\frac{D(\ )}{dt} = \frac{\partial(\ )}{\partial t} + U_o \frac{\partial(\ )}{\partial x} \qquad (1)$$

Taylor's hypothesis states that for all but the smallest values of U_o, the second term dominates and the first may be ignored. The lower limit of U_o is comparable to the convection velocity (Dobrolenskiy[4]) and the vehicle velocity can be as low as one-third of the wind speed for good correlation (Etkin[5]). It is to be noted that the only vehicles capable of less than this flight velocity are LTA and VTOL craft, and then only when they are convected downwind with the airmass. For the small portion of the flight envelope in which the theory does not hold, the forces generated on the structure are small and do not present a problem.

Turbulence Organization

What happens at one location in the atmosphere affects conditions at other locations. Fluidynamicists characterize this interdependence by the use of stress and strain relationships in the fluid. This techniques has been applied to turbulence (Ferzinger[6]) with some success in predicting the actual velocity field for a boundary layer type flow.

For flight vehicle analysis, Ribner's[7] specification of the velocity field by the spectral decomposition of the three-dimensional homgeneous vector field is more convenient than the expression of interdependence. Figure 2 shows an airship flying through a two-dimensional, sinusoidal wave of shearing motion.

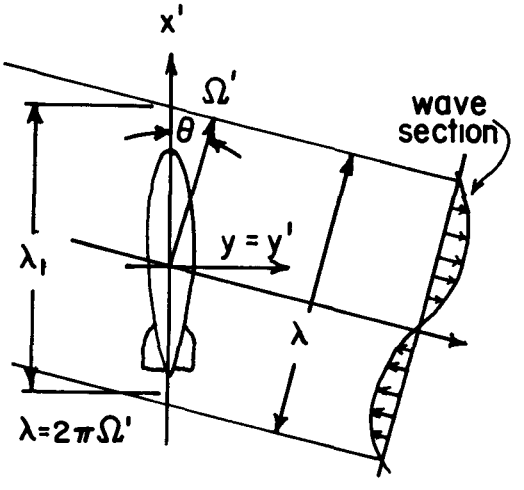

Fig. 2 Derived Gust Velocity

The velocity change from the lateral gust component mean is given as:

$$dv_g(x',y') = e^{i(\Omega_1 x + \Omega_2 y)} dc_2 \qquad (2)$$

where Ω_1 and Ω_2 are the wave number components in the x' and y' directions respectively, and c_2 is the complex lateral component amplitude. When the vehicle, with velocity U , penetrates the field, the coordinates become x' = x + Uo t, and y' = y in the body-fixed system. Equation (2) then becomes,

$$dv_g(x,y) = e^{i\Omega_1 U_o t}\, e^{i(\Omega_1 x + \Omega_2 y)} \qquad (3)$$

The air velocity over the vehicle is then periodic with wavelengths of $(2\pi/\Omega_{1,2})$ and frequencies of $(\Omega_{1,2}U_o/2)$. The total field is composed of the superposition of these spectral components, much as a Fourier series represents a random scalar.

Probability Distribution and Spectra

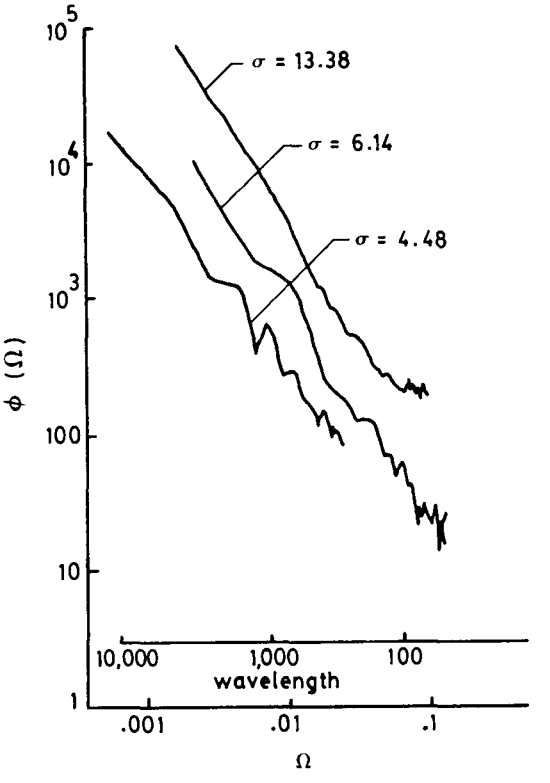

Fig. 3 Power Spectra of Vertical Gust

The power spectral density of a time varying function, X(t), is defined (in terms of wave number) as

$$\Phi(\Omega) = \lim_{\substack{\Delta\Omega \to \\ T \to \infty}} \frac{1}{T\Delta\Omega} \int_0^T X(t,\Omega,\Delta\Omega)\, dt \qquad (4)$$

where $\phi(\Omega)$ is expressed in (ft/sec) per (radians/ft), and T is the duration over which X(t) is measured. This value may be computed by taking the autocorrelation function $R(\tau)$ and performing a Fourier transformation,

Figure 3, (Ref. 8), shows the spectra of three different meteorological conditions. Although these depictions vary in detail, they all exhibit the same decreasing trend at the higher frequencies. Inasmuch as the values of the spectra at higher frequencies contribute little to the response of the aircraft, only the area under the actual curve is measured.

From the analysis of a large number of samples, it is apparent that the probability distribution is non-Gaussian (Ref 9), with the extreme high and extreme low values of intensity occurring more frequently than predicted by a normal distribution. In order to account for the large gusts omitted by the use of the linear system models (normal distribution related), the (1 - cosine) method can be used.

The two most widely used Gaussian models are the Dryden spectrum, first used to define the turbulence spectra in wind tunnels, and the von Karman spectrum. While the Dryden model is less complex, it is, in turn, less accurate, and as a result, the von Karman spectrum

$$\phi(\Omega) = \frac{1}{2\pi}\int_{-\infty}^{\infty} R(\tau)\, e^{i\Omega\tau}\, \tau \qquad (5)$$

is used almost universally.

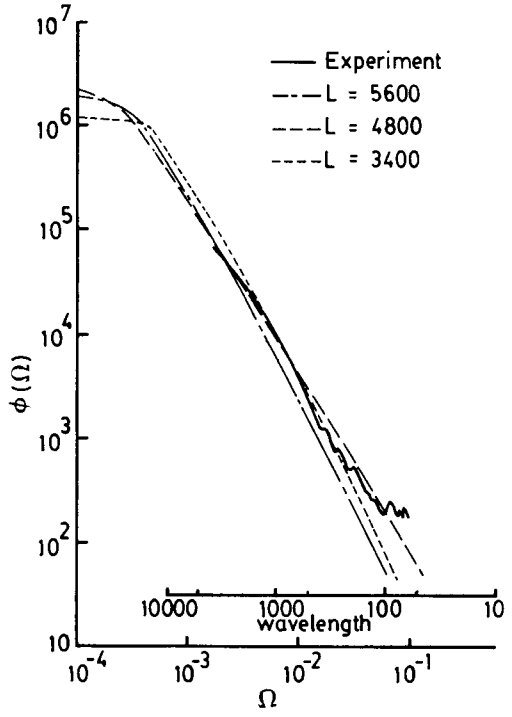

Fig. 4 von Karman Spectra - Severe Storm

$$\phi_{22}(\Omega) = \frac{\sigma^2 L}{\pi} \frac{1 + \frac{8}{3}(1.339\tilde{L}\Omega)^2}{[1 + (1.339\tilde{L}\Omega)^2]^{11/10}} \qquad (6)$$

In Equation (6), σ is the RMS turbulence intensity, and $\tilde{L}$ is the "scale length" - a measure of the average eddy size. Figure (4) is a plot of one set of experimental data along with the predicted turbulence spectra for severe storm conditions for various values of $\tilde{L}$.

Method of Analysis

The Model

The aerodynamic model used in this analysis is the same as used by DeLaurier and Hui (Ref 10) except that it is applied for the lateral case. The assumptions are:

i) The vehicle is perfectly rigid, flying at a constant velocity U_o through a constant density .

ii) The motions are described for the lateral case only.

iii) The control provided by the rudder deflection is linearly proportional to the yaw angle (Ψ), i.e.,

$\Delta C_{yc} = k_c \Psi$.

This last assumption relates the helmsman using greater control the more off-heading he is perturbed, an assumption in keeping with operational practice.

The turbulence model is the von Karman spectra, described previously, and it is composed of horizontal gusts only, either u_g or v_g depending of the heading of the airship relative to the mean wind direction.

Turbulence Component Forces

After the method of Jones and DeLaurier [11], the change with respect to sideslip of the normal force on a hull segment of length $d\zeta$ is (See Figure 5)

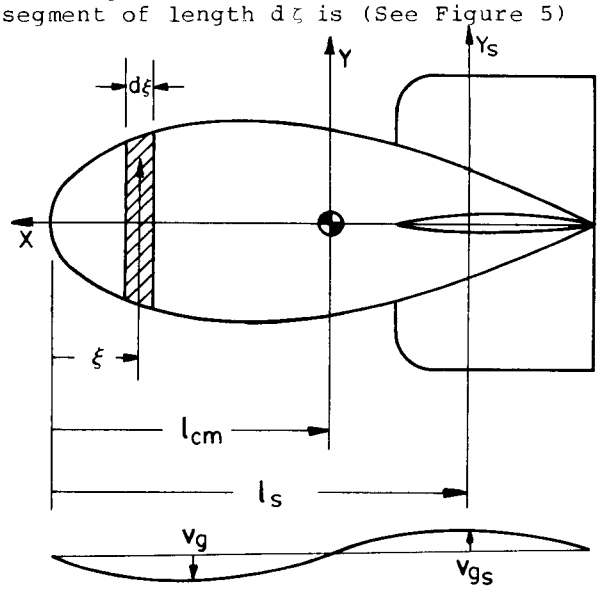

Fig. 5 Airship Loads from Turbulence

$$F_h = \tfrac{1}{2}\rho U_o^2 [K \sin(2\theta) \cos(\tfrac{\theta}{2}) \frac{dA}{d\xi} d\xi + (C_{d_c})_h \sin(\theta) \sin|\theta| 2r d\xi] \quad (7)$$

where: K is the potential cross-flow factor (Ref 11)

θ is the angle between the hull centerline and U_o.

A is the cross-sectional hull area.

In addition, if the undisturbed value of the sideslip, β_o, is assumed to be zero, and since, for small values of v_g, $d\beta = v_g/U_o$, Equation (7) reduces to

$$(dY_g)_h = \rho U_o^2 K \frac{dA}{d\xi} \frac{v_g}{U_o} d\xi \quad (8)$$

In a similar manner, the stabilizer forces are given,

$$(Y_g)_s = \rho \frac{U_o^2}{2} S_s (C_{L_\alpha}^*)_s H(k_s)_s \frac{(v_g)_s}{U_o} \quad (9)$$

where: $H(k_s)$ is the generalized Sears Function as given by Filotas (Ref. 12)

$k_s = \omega \bar{c}/2U_o$, the "reduced frequency" of the fin.

$(v_g)_s$ is the gust velocity at the fin mid-chord.

The thrusters used to drive the airship produce a side force when acted on by turbulence. Each thruster contribution adds to the total force and moment, and can be described, for the jth thruster-rotor combination as,

$$(Y_g)_{T_j} = -\rho \frac{U_o^2}{2} S_{T_j} (C_{y_\beta})_{T_j} \frac{(v_{g_T})_j}{U_o} \quad (10)$$

$$(L_g)_{T_j} = (Y_g)_{T_j} (h_{cm} - h_{T_j}) \quad (11)$$

$$(N_g)_{T_j} = (Y_g)_{T_j} (l_{cm} - l_{T_j}) \quad (12)$$

Equations (11) and (12) assume that the rotors are arranged symmetrically about the x-z plane so that moments due to rotor offset in the y-direction cancel out.

Aero Forces and Moments due to Motion

The element force on the hull is,

$$(dY_w)_h = \rho U_o^2 K \frac{dA}{d\xi} d\xi \frac{v(\xi)}{U_o} + \rho A [k_2 \frac{\partial v(\xi)}{\partial t} + U_o r k_1] d\xi \quad (13)$$

where k_1 and k_2 are the longitudinal and horizontal apparent mass coefficients and

$$v(\xi) = v - r(l_{cm} - \xi) \quad (14)$$

For the fins (Stabilizers) one has,

$$(Y_w)_s = -\rho \frac{U_o^2}{2} S_s (C_{y_\beta})_s \frac{v_s}{U_o} + (C_{y_r})_s^{ac} \frac{\bar{c}r}{2U_o} + (C_{y_{\dot\beta}}) \frac{\bar{c}\dot{v}_s}{2U_o^2} \quad (15)$$

where: $v_s = v - r(l_{cm} - l_s)$
$\dot{v}_s = \dot{v} - r(l_{cm} - l_s)$

The moments for the fins are

$$(L_w)_s = (Y_w)_s (h_{cm})_s \quad (16)$$

$$(N_w)_s = \tfrac{1}{2}\rho U_o^2 S_s \bar{c}_s (C_{n_r})_s^{ac} \frac{\bar{c}r}{2U_0} \quad (17)$$

(The superscript 'ac' indicates that the quantity in parenthesis is taken about the aerodynamic center of the fin.)

Thruster forces and moments are given by,

$$(Y_w)_{T_j} = -\rho \frac{U_o^2}{2} S_{T_j} (C_{y_\beta})_{T_j} \frac{(v_T)_j}{U_o} \quad (18)$$

$$(L_w)_{T_j} = (Y_w)_{T_j} (h_{cm} - h_{T_j}) \quad (19)$$

$$(N_w)_{T_j} = (Y_w)_{T_j} (l_{cm} - l_{T_j}) \quad (20)$$

where: $(v_T)_j = v - r(l_{cm} - l_{T_j}) - p(h_{cm} - h_{T_j})$

Inertial Reaction to Forces and Moments

The forces and moments arising as reactions to the airship motion are the negative of the forces and moments that generate the airship translational and angular velocities and accelerations so as to produce a state of dynamic equilibrium.

For the hull,

$$(dY_m)_h = -\ddot{y}'(\xi)(d_m)_h \quad (21)$$

where $\ddot{y}' = \dot{v} + \dot{r}(l_{cm} - \zeta) + U_o r$

$$(dL_m)_h = -dI_{xx}\dot{p} + dI_{xz}\dot{r} \quad (22)$$

$$(dN_m)_h = -dI_{zz}\dot{r} + dI_{xz}\dot{p} \quad (23)$$

For the stabilizers,

$$(Y_m)_s = -\ddot{y}'_s m_s \quad (24)$$

$$(N_m)_s = -(I_{zz})_s \dot{r} + (I_{zx})_s \dot{p} \quad (25)$$

$$(L_m)_s = -(I_{xx})_s \dot{p} + (I_{zx})_s \dot{r} \quad (26)$$

where the moments and products of inertia (and the inertias of the differential elements) include all structure, air and gas contained in the airship.

Bouyancy and Control Terms

The perturbation equation of the bouyant force is,

$$(dY_b)_h = (\rho g A d \quad - gdm) \cos \alpha_o \, d\phi \quad (27)$$

Control force is due to rudder deflection and acts through the aerodynamic center of the fin,

$$(Y_c)_s = \rho \frac{U_o^2}{2} S_s \, k_c \, \psi \quad (28)$$

Shear Force, Bending and Twisting Moment

The shear force of the hull at a station (l) may be obtained by summing the sideforce values from the nose of the airship to Station (l), including the number of rotors, a, forward of Station (l)

$$S(l) = \int_0^l (dy)_h + \sum_{j=1}^{a} [(Y_g)_{T_j} + (Y_w)_{T_j}] \quad (29)$$

where: $(dY)_h = (dY_g)_h + (dY_w)_h + (dY_b)_h + (dY_m)_h$

The bending moment at (l), measured along the centerline, is,

$$BM(l) = \int_0^l (l_{cm}-\xi)(dy)_h + \int_0^l (dN_m)_h + \sum_{j=1}^{a} (l-l_{T_j})[(Y_g)_{T_j} + (Y_w)_{T_j}] \quad (30)$$

And the twisting moment at Station (l) is,

$$TM(l) = -\int_0^l h_{cm}(\xi)(dY)_h + \int_0^l (dL_m)_h + \int_0^l (dL_{mg})_h - \sum_{j=1}^{a} (h_{T_j})[(Y_g)_{Tj} + (Y_w)_{T_j}] \quad (31)$$

The term $(dL_{mg})_h$ is the torque contribution due to the center of gravity being offset from the central axis, as shown in Figure 6, where the term $(dL_{mg})_h$ is calculated from

$$(dL_{mg})_h = h_{cm} g \, dm \, \phi \cos \alpha_o \quad (32)$$

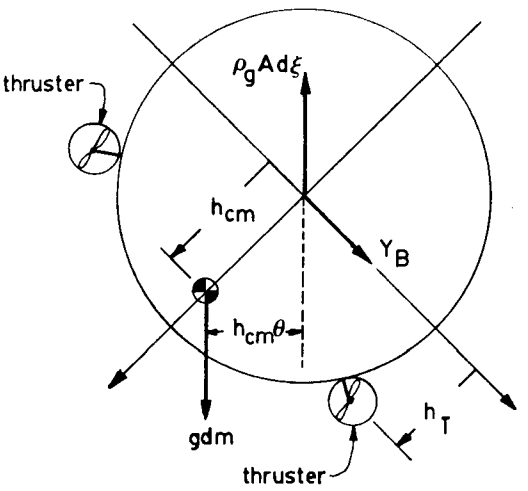

Fig. 6 Bouyancy Forces and Moments

Flight Dynamics

Dynamic Stability

The equations for Lateral Dynamic Stability, from DeLaurier and Schneck , are linear and can be written in a matrix form as:

$$[\tilde{C}] \begin{bmatrix} \hat{v} \\ \hat{r} \\ \hat{p} \\ \hat{\phi} \\ \hat{\psi} \end{bmatrix} - [\tilde{D}] \begin{bmatrix} D\hat{v} \\ D\hat{r} \\ D\hat{p} \\ D\hat{\phi} \\ D\hat{\psi} \end{bmatrix} = 0 \quad (33)$$

where: v is the y-direction translation
r is the rotation rate about the z-axis
p is the rotation rate about the x-axis
ϕ is the roll angle
ψ is the yaw angle

The matrices $\tilde{C}$ and $\tilde{D}$ are given by,

$$[\tilde{C}] = \begin{bmatrix} C_{y\beta} & (C_{yr}-2\mu) & C_{yp} & (\hat{mg}-\hat{B}) \cos\alpha_o & -k \\ C_{n\beta} & C_{nr} & C_{np} & -x_{bB} \cos\alpha_o & j^* \\ C_{l\beta} & C_{lr} & C_{lp} & -z_{bB} \cos\alpha_o & h^* \\ 0 & \tan\alpha_o & 1 & 0 & 0 \\ 0 & \sec\alpha_o & 0 & 0 & 0 \end{bmatrix} \quad (34)$$

where:
$j^* = (l_s - l_{cm})(k_c\sqrt{c})$
$h^* = h_{cm}/k_c\sqrt{c})$

$$[\tilde{D}] = \begin{bmatrix} (2\mu - C_{y\dot{\beta}}) & -C_{y\dot{r}} & -C_{y\dot{p}} & 0 & 0 \\ -C_{n\dot{\beta}} & (I_{zz} - C_{n\dot{r}}) & -(I_{xz} + C_{n\dot{p}}) & 0 & 0 \\ -C_{l\dot{\beta}} & -(I_{xz} + C_{l\dot{r}}) & (I_{xx} - C_{l\dot{p}}) & 0 & 0 \\ 0 & 0 & 0 & 1 & 0 \\ 0 & 0 & 0 & 0 & 1 \end{bmatrix} \quad (35)$$

This system of equations may be solved by assuming a solution of the order of

$$\hat{v} = \hat{V} e^{i\hat{\partial}\hat{t}} \qquad \hat{p} = \hat{p} e^{i\partial\hat{t}} \quad \text{etc}$$

which, when substituted into Equation (32), becomes,

$$[\tilde{C} - i\hat{\sigma}\tilde{D}] \begin{bmatrix} \hat{V} \\ \hat{R} \\ \hat{P} \\ \hat{\phi} \\ \hat{\psi} \end{bmatrix} = 0 \qquad (36)$$

where $\hat{\sigma}$ is the non-dimensional stability root. This is an eigenvalue problem and a computer is used to find the eigenvalues (stability roots) and eigenvectors (model vectors) for the control gains considered.

Turbulence Forcing Functions

By integrating the sinusoidal turbulence model with Gaussian statistics from the nose to the hull/fin intersection, and adding the contribution of the fins and the thrusters, the complete forcing functions can be found.

Lateral force

$$Y_g = \int d(Y_g)_h + \Sigma[(Y_g)_{T_j} + (Y_g)_s] \qquad (37)$$

Yawing moment

$$N_{g_{nose}} = \int d(Y_g)_h + \sum_{j=1}^{a} [(l_T)_j (Y_g)_{T_j}] + l_s (Y_g)_s \qquad (38)$$

Rolling moment

$$L_g = - h_{cm} Y_g \qquad (39)$$

These equations may be non-dimensionalized according to,

$$Y_g = \tfrac{1}{2} U_o^2 S G_Y \quad (L_g, N_g) = \tfrac{1}{2} U_o^2 S \bar{c} (G_l, G_n) \qquad (40)$$

and the non-dimensional equations can be expressed as

$$G_Y = G_{Y_\gamma} \gamma \qquad G_l = G_{l_\gamma} \gamma \qquad G_n = G_{n_\gamma} \gamma \qquad (41)$$

where: $\gamma = \Gamma \exp(i\omega t) = \Gamma \exp(ik\hat{t})$ and $k = \bar{c}\omega / 2U_o$

Gy_γ, Gl_γ and Gn_γ are the turbulent forcing functions.

Motion Response Transfer Functions

Using the functions of Equation (41) as forcing functions on the right-hand side of Equation (36), and dividing through by Γ gives,

$$[\tilde{C} - ik\tilde{D}] \begin{matrix} \hat{V}/\Gamma \\ \hat{R}/\Gamma \\ \hat{P}/\Gamma \\ \hat{\phi}/\Gamma \\ \hat{\psi}/\Gamma \end{matrix} \begin{matrix} Gy_\Gamma \\ Gn_\Gamma \\ Gl_\Gamma \\ 0 \\ 0 \end{matrix} \qquad (42)$$

Solution of Equation (42) for specific reduced frequencies, k, or spectral wave numbers, Ω, and fixed stable control gains, k_c, allows calculation of the expressions necessary for the solution of distributed force loading and moments.

Load Response Transfer Functions

The turbulence loading may be obtained by substituting the Gaussian equation into Equations (7) through (11) and dividing through by γ. A complete listing of the Load Response Transfer Functions is to be found in Reference 14.

The aerodynamic-reaction loading is obtained by replacing the motion variables in Equations (13) through (19) with the derived motion response transfer functions, and the inertial-reaction and bouyancy loading transfer functions are similarly obtained from Equations (20) through (27).

Shear Force, Bending and Twisting Moment Transfer Functions

The shear force, bending and twisting moment transfer functions are obtained by using Equations (29), (30) and (31), respectively, and a check on the analytical model is obtained by insuring that the net shear force, bending and twisting moments equal zero.

Response to Atmospheric Turbulence

Once the force and moment transfer function coefficients are known, the turbulence statistics can be applied to obtain estimates of airship lifetime and failure probability. When dealing with the lateral aerodynamic case, two power sprectral functions, ϕ_{11} and ϕ_{22} must be considered. ϕ_{11} is used when the flight direction is perpendicular to the mean wind and ϕ_{22} is used when the wind direction is parallel. Several methods may be used to determine the behavior of the airship. The Root-Mean-Square Method can be obtained by using the RMS transfer function multiplied by the spectrum, if Gaussian. Response to various conditions can be evaluated using appropriate values for $\hat{\sigma}$ and L in the equation for ϕ_{11},

$$\phi_{11}(\Omega) = \frac{\sigma^2 \tilde{L}}{\pi} \frac{2}{[1+(1.339\tilde{L}\Omega)^2]^{5/6}} \qquad (43)$$

and choosing either ϕ_{11} or ϕ_{22} according to the flight direction.

The Mission Analysis Method[5], is a technique for estimating the probable lifetime of a flight vehicle, based on the probability distribution of encountering turbulence in representative flight operations. The probable lifetime is the inverse of the number of exceedences of a stated bending moment coefficient in a stipulated time, where the number of exceedences is given as,

$$N(x) = \Sigma t N_o \left[p_1 \exp\left(\frac{-|x - x_{ref}|}{b_1 \bar{A}} \right) + p_2 \exp\left(\frac{-|x - x_{ref}|}{b_2 \bar{A}} \right) \right] \qquad (44)$$

where: x = max bending moment coeff. at a given station
x_{ref} = value of x in one-g flight
$N(x)$ = average number of exceedences per unit time
N_o = number of zero crossings of x per unit time
$\bar{A}$ = $[(C_{BM})_{rms}/\sigma]/\gamma_{rms}$
t = fraction of time in mission segment
p_i = probability values
b_i = intensity levels.
Values of p_i and b_i may be found in Table I of Ref. 14.

DeLaurier and Hui also include Failure-Probability Analysis and the "Mil-Spec Storm" Analysis in their paper. There are other techniques, such as the Design Envelope Analysis that are available and well documented.

Numerical Example

A numerical example using the USS AKRON (ZRS-4) has been used to validate this work. 1,000 foot altitude and a flight velocity of 123 feet per second were chosen, as was a neutral bouyancy. The hull cross-flow factor was determined as K = 0.93225 and the stabilizer efficiency was calculated to be 0.2600.

The forcing functions were obtained from Equations (37) through (41) and are plotted in Figure 7. The peaks in all of the curves occur at a wave number of about 0.008, which corresponds to the length of the airship.

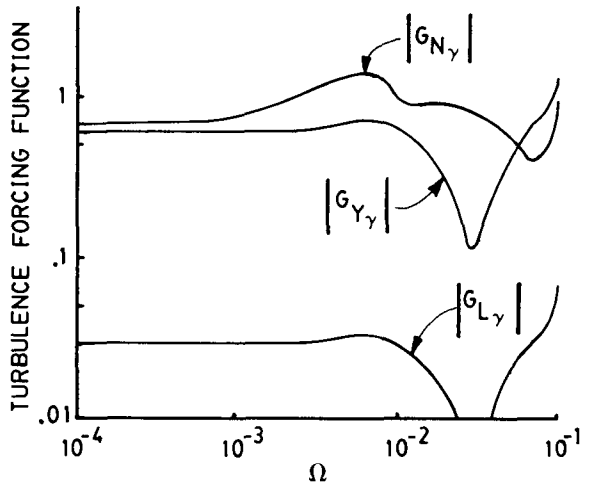

Fig. 7 Turbulence Forcing Functions

Equation (42) was solved to obtain the motion response transfer functions for control gains of 0.2, 1.0 and 2.0. Results were obtained for side slip, yaw, yaw rate, roll, and roll rate. A typical response, that for yaw response, is shown in Figure 8.

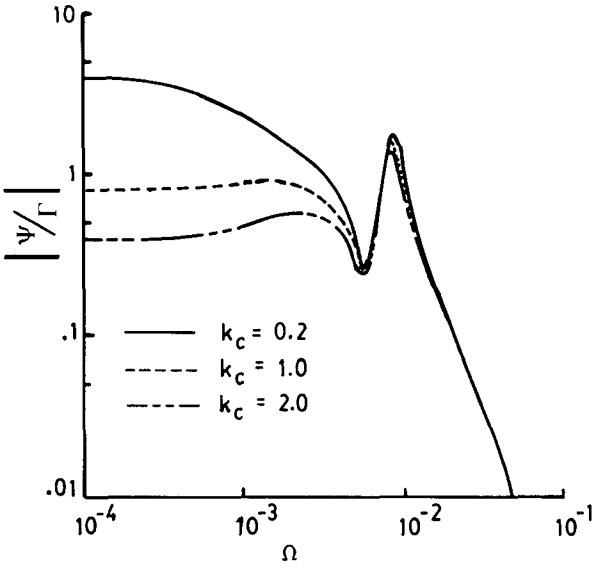

Fig. 8 Yaw Response

The most significant feature of the responses is the peak at a wave number of 0.008. For the lateral case the control gain does not change this peak significantly.

Finally, the load response transfer functions were calculated for a wave number of .009 and a control gain of 0.2. The bending moment coefficient response is similar to that of the yaw response except that the location of the peak load shifts aft for the shear force and twisting moment cases.

Conclusions and Summary

This analysis, which is an extension of the work by DeLaurier and Hui, is subject to the same restrictions. That is, it is limited to small perturbations in order to allow a linear analysis useable with power spectral methods, and its ability to make precise predictions of loading is somewhat questionable. Nevertheless, it is a valuable tool in understanding the response to an initial disturbance, and when used as the aerodynamic input to the various statistical methods, can yield important design and operational insight.

The limited effectiveness of the simple control model used, which is analogous to cueing steering response to a compass, is demonstrated. It would appear that a yaw rate feedback system would be more useful, particularly as a means of gust alleviation.

As with the longitudinal case, control gain plays an important role in the expected lifetime of an airship. Even the first order yaw control used in this analysis will contribute to increased survivability due to the reduction of loads at low wave numbers.

Inasmuch as no aircraft has ever flown through one-dimensional turbulence, examination of combined longi-

tudinal and lateral motion needs to be made. Coupling the motion would lead to a much better understanding of the true action of the airship in turbulence.

Finally, experimental verification of the response solutions, both longitudinal and lateral, is necessary to provide a quantitative base for these calculations. This could be accomplished in-flight or in a wind tunnel.

Acknowledgement

This research was supported by funding from the United States Coast Guard.

List of References

1. Burgess, C. P., Airship Design, pp. 99-100, Ronald Press, 1927.

2. Press, R. and Meadows, M. T., A Reevaluation of Gust-Load Data Statistics for Applications in Spectral Calculations, NACA TN 3540, 1955.

3. Calligeros, J. M. and McDavitt, P. W., Response and Loads on Airships due to Discrete and Random Gusts, MIT Aeroelastic and Structures Research Lab. Tech. Rpt. 72-1, Cambridge, Mass, February 1958

4. Dobrolenskiy, Yu. P., Flight Dynamics in Moving Air, NASA TT F-600, July 1971.

5. Etkin, B., The Turbulent Wind and its Effect on Flight, UTIAS Review No. 44, University of Toronto Institute for Aerospace Studies, August 1980.

6. Ferzinger, J. H., Large-Eddy Simulation, Lecture presented at the AIAA Professional Study Seminar on Turbulence Modeling, Palo Alto, California, 20-21 June 1981.

7. Ribner, H. S. Spectral Theory of Buffeting and Gust Response; Unification and Extension, Journal of Aero. Sci., Vol. 23, No. 12, 1956.

8. Houbolt, J. C., Steiner, R., and Pratt, K. G., Dynamic Response of Airplanes to Atmospheric Turbulence (Including Flight Data on Input and Response), NASA TR-R-199, 1964.

9. Houbolt, J. C., Atmospheric Turbulence, AIAA Journal, Vol. 11, No. 4, April 1973.

10. DeLaurier, J. D. and Hui,, K. C. K., Airship Survivability in Atmospheric Turbulence, AIAA Paper 81-1323, July 1981.

11. Jones, S. P. and DeLaurier, J. D., Aerodynamic Estimation Techniques for Aerostats and Airships, AIAA Paper 81-1339, July 1981.

12. Filotas, L. T., Approximate Transfer Functions for Large Aspect Ratio Wings in Turbulent Flow, AIAA J. of Aircraft, Vol. 8, No, 6, June 1971

13. Ribner, H. S., Propellers in Yaw, NACA Report No. 820, 1945.

14. Wrobleski, J. J. Jr., The Lateral Response of an Airship to Turbulence, Master of Science Thesis, Naval Postgraduate School, December 1981.

15. DeLaurier, J. D. and Schenck, D. M., Airship Dynamic Stability, AIAA Paper 79-1591, July 1977.